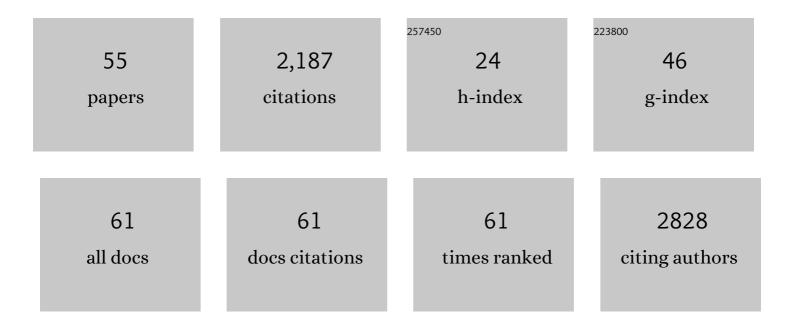
Tom Willhammar

List of Publications by Year in descending order

Source: https://exaly.com/author-pdf/536011/publications.pdf Version: 2024-02-01



#	Article	IF	CITATIONS
1	ZSM-5 Zeolite Single Crystals with <i>b</i> -Axis-Aligned Mesoporous Channels as an Efficient Catalyst for Conversion of Bulky Organic Molecules. Journal of the American Chemical Society, 2012, 134, 4557-4560.	13.7	264
2	Structure and catalytic properties of the most complex intergrown zeolite ITQ-39 determined by electron crystallography. Nature Chemistry, 2012, 4, 188-194.	13.6	178
3	Gel-based morphological design of zirconium metal–organic frameworks. Chemical Science, 2017, 8, 3939-3948.	7.4	177
4	Luminescent CulnS ₂ Quantum Dots by Partial Cation Exchange in Cu _{2–<i>x</i>} S Nanocrystals. Chemistry of Materials, 2015, 27, 621-628.	6.7	127
5	A Robust and Biocompatible Bismuth Ellagate MOF Synthesized Under Green Ambient Conditions. Journal of the American Chemical Society, 2020, 142, 16795-16804.	13.7	115
6	A Titanium(IV)â€Based Metal–Organic Framework Featuring Defectâ€Rich Tiâ€O Sheets as an Oxidative Desulfurization Catalyst. Angewandte Chemie - International Edition, 2019, 58, 9160-9165.	13.8	99
7	A priori control of zeolite phase competition and intergrowth with high-throughput simulations. Science, 2021, 374, 308-315.	12.6	90
8	A New Aluminosilicate Molecular Sieve with a System of Pores between Those of ZSM-5 and Beta Zeolite. Journal of the American Chemical Society, 2011, 133, 9497-9505.	13.7	86
9	Synthesis Design and Structure of a Multipore Zeolite with Interconnected 12- and 10-MR Channels. Journal of the American Chemical Society, 2012, 134, 6473-6478.	13.7	75
10	EMM-23: A Stable High-Silica Multidimensional Zeolite with Extra-Large Trilobe-Shaped Channels. Journal of the American Chemical Society, 2014, 136, 13570-13573.	13.7	71
11	A Tunable Multivariate Metal–Organic Framework as a Platform for Designing Photocatalysts. Journal of the American Chemical Society, 2021, 143, 6333-6338.	13.7	69
12	Local Crystallinity in Twisted Cellulose Nanofibers. ACS Nano, 2021, 15, 2730-2737.	14.6	53
13	Structural Determination of Ordered Porous Solids by Electron Crystallography. Advanced Functional Materials, 2014, 24, 182-199.	14.9	51
14	Self-Assembly of Pluronic F127—Silica Spherical Core–Shell Nanoparticles in Cubic Close-Packed Structures. Chemistry of Materials, 2015, 27, 5161-5169.	6.7	47
15	Three-dimensional electron diffraction for porous crystalline materials: structural determination and beyond. Chemical Science, 2021, 12, 1206-1219.	7.4	44
16	Synthesis and characterization of pure silica zeolite beta obtained by an aging–drying method. Microporous and Mesoporous Materials, 2011, 143, 196-205.	4.4	40
17	Structure and vacancy distribution in copper telluride nanoparticles influence plasmonic activity in the near-infrared. Nature Communications, 2017, 8, 14925.	12.8	38
18	A Titanium(IV)â€Based Metal–Organic Framework Featuring Defectâ€Rich Tiâ€O Sheets as an Oxidative Desulfurization Catalyst. Angewandte Chemie, 2019, 131, 9258-9263.	2.0	37

TOM WILLHAMMAR

#	Article	IF	CITATIONS
19	A Novel Porous Tiâ€Squarate as Efficient Photocatalyst in the Overall Water Splitting Reaction under Simulated Sunlight Irradiation. Advanced Materials, 2021, 33, e2106627.	21.0	35
20	Facile Processing of Transparent Wood Nanocomposites with Structural Color from Plasmonic Nanoparticles. Chemistry of Materials, 2021, 33, 3736-3745.	6.7	32
21	Microcavity-like exciton-polaritons can be the primary photoexcitation in bare organic semiconductors. Nature Communications, 2021, 12, 6519.	12.8	32
22	Transmission electron microscopy as an important tool for characterization of zeolite structures. Inorganic Chemistry Frontiers, 2018, 5, 2836-2855.	6.0	29
23	Mesoscale Transformation of Amorphous Calcium Carbonate to Porous Vaterite Microparticles with Morphology Control. Crystal Growth and Design, 2019, 19, 5075-5087.	3.0	27
24	Introducing the crystalline phase of dicalcium phosphate monohydrate. Nature Communications, 2020, 11, 1546.	12.8	26
25	Hierarchical micro-reactor as electrodes for water splitting by metal rod tipped carbon nanocapsule self-assembly in carbonized wood. Applied Catalysis B: Environmental, 2020, 264, 118536.	20.2	25
26	Single-walled zeolitic nanotubes. Science, 2022, 375, 62-66.	12.6	25
27	Synthesis and Structure of a 22 × 12 × 12 Extra-Large Pore Zeolite ITQ-56 Determined by 3D Electron Diffraction. Journal of the American Chemical Society, 2021, 143, 8713-8719.	13.7	22
28	Structure of the active pharmaceutical ingredient bismuth subsalicylate. Nature Communications, 2022, 13, 1984.	12.8	22
29	Influence of Synthesis Routes on the Crystallography, Morphology, and Electrochemistry of Li ₂ MnO ₃ . ACS Applied Materials & Interfaces, 2020, 12, 5939-5950.	8.0	20
30	Gas sorption properties and kinetics of porous bismuth-based metal-organic frameworks and the selective CO2 and SF6 sorption on a new bismuth trimesate-based structure UU-200. Microporous and Mesoporous Materials, 2022, 329, 111548.	4.4	19
31	NH3-SCR catalysts for heavy-duty diesel vehicles: Preparation of CHA-type zeolites with low-cost templates. Applied Catalysis B: Environmental, 2022, 303, 120928.	20.2	18
32	Tunable CHA/AEI Zeolite Intergrowths with A Priori Biselective Organic Structureâ€Directing Agents: Controlling Enrichment and Implications for Selective Catalytic Reduction of NOx. Angewandte Chemie - International Edition, 2022, 61, .	13.8	18
33	Postsynthetic High-Alumina Zeolite Crystal Engineering in Organic-Free Hyper-Alkaline Media. Chemistry of Materials, 2017, 29, 629-638.	6.7	17
34	Synthesis of Al–Si-beta and Ti–Si-beta by the aging–drying method. Microporous and Mesoporous Materials, 2012, 150, 38-46.	4.4	15
35	High-Throughput Synthesis and Structure of Zeolite ZSM-43 with Two-Directional 8-Ring Channels. Inorganic Chemistry, 2017, 56, 8856-8864.	4.0	15
36	A structure determination protocol based on combined analysis of 3D-ED data, powder XRD data, solid-state NMR data and DFT-D calculations reveals the structure of a new polymorph of <scp>l</scp> -tyrosine. Chemical Science, 2022, 13, 5277-5288.	7.4	15

TOM WILLHAMMAR

#	Article	IF	CITATIONS
37	3D reconstruction of atomic structures from high angle annular dark field (HAADF) STEM images and its application on zeolite silicalite-1. Dalton Transactions, 2014, 43, 14158-14163.	3.3	12
38	EMM-25: The Structure of Two-Dimensional 11 × 10 Medium-Pore Borosilicate Zeolite Unraveled Using 3D Electron Diffraction. Chemistry of Materials, 2021, 33, 4146-4153.	6.7	11
39	Solving complex open-framework structures from X-ray powder diffraction by direct-space methods using composite building units. Journal of Applied Crystallography, 2013, 46, 1094-1104.	4.5	10
40	A Stacking Faults-Containing Silicogermanate with 24-Ring Channels and Unbranched Zweier Silica Double Chains. Crystal Growth and Design, 2012, 12, 3714-3719.	3.0	9
41	Post-synthesis bromination of benzene bridged PMO as a way to create a high potential hybrid material. Microporous and Mesoporous Materials, 2016, 236, 244-249.	4.4	9
42	Influence of the substitution pattern of four naphthalenedicarboxylic acids on the structures and properties of group 13 metal–organic frameworks and coordination polymers. Dalton Transactions, 2020, 49, 4861-4868.	3.3	9
43	Small Pore Aluminosilicate EMM-37: Synthesis and Structure Determination Using Continuous Rotation Electron Diffraction. Inorganic Chemistry, 2019, 58, 12854-12858.	4.0	7
44	Structure–property relationships in organic battery anode materials: exploring redox reactions in crystalline Na- and Li-benzene diacrylate using combined crystallography and density functional theory calculations. Materials Advances, 2021, 2, 1024-1034.	5.4	7
45	Metal–biomolecule frameworks (BioMOFs): a novel approach for "green―optoelectronic applications. Chemical Communications, 2022, 58, 677-680.	4.1	7
46	A Germanate with a Collapsible Open-Framework. Crystal Growth and Design, 2016, 16, 6967-6973.	3.0	4
47	Detailed Structural Survey of the Zeolite ITQ-39 by Electron Crystallography. Crystal Growth and Design, 2017, 17, 1910-1917.	3.0	4
48	Design and degradation of permanently porous vitamin C and zinc-based metal-organic framework. Communications Chemistry, 2022, 5, .	4.5	4
49	Phase Transformation Behavior of a Twoâ€Dimensional Zeolite. Angewandte Chemie - International Edition, 2019, 58, 10230-10235.	13.8	3
50	An adsorbent with flexible nanoscopic pores. Science, 2022, 376, 457-458.	12.6	3
51	Aluminosilicate Zeolite EMM-28 Containing Supercavities Determined by Continuous Rotation Electron Diffraction. Inorganic Chemistry, 2022, 61, 11103-11109.	4.0	2
52	Scan Strategies for Electron Energy Loss Spectroscopy at Optical and Vibrational Energies in Perylene Diimide Nanobelts. Microscopy and Microanalysis, 2019, 25, 1738-1739.	0.4	1
53	Phase Transformation Behavior of a Twoâ€Dimensional Zeolite. Angewandte Chemie, 2019, 131, 10336-10341.	2.0	1
54	Tunable CHA/AEI Zeolite Intergrowths with A Priori Biselective Organic Structureâ€Directing Agents: Controlling Enrichment and Implications for Selective Catalytic Reduction of NOx. Angewandte Chemie, 0, , .	2.0	1

#	Article	IF	CITATIONS
55	Two-Dimensional Cationic Aluminoborate as a New Paradigm for Highly Selective and Efficient Cr(VI) Capture from Aqueous Solution. Jacs Au, 2022, 2, 1669-1678.	7.9	1